Disposition of intracellular cholesterol in human fibroblasts

Yvonne Lange

Departments of Pathology and Biochemistry, Rush-Presbyterian-St. Luke's Medical Center, Chicago, IL 60612-3864

Abstract We have examined the intracellular distribution of unesterified cholesterol in cultured human fibroblasts. Intact cells were treated with cholesterol oxidase to selectively transform cell surface cholesterol to cholestenone. Isopycnic centrifugation of homogenates showed that the cholestenone had a peak buoyant density of 1.13 g/cm^3. The ~10% of total cholesterol which remained unoxidized was distributed in two peaks of roughly equal size: a sharp peak at approximately 1.09 g/cm^3 and a broad peak centered at 1.18 g/cm^3. When intact cells were incubated with exogenous [^{3}H]cholesterol, the radiolabel entered the nonoxidizable pool in a temperature-dependent fashion with a half time of 3 h at 37°C. This label initially was associated with the dense but not the buoyant peak of nonoxidized cholesterol. After 40 h, the buoyant peak also became labeled; both peaks then had a specific activity slightly less than the surface cholestenone. The buoyant density of the unoxidized cholesterol did not coincide with markers for the Golgi apparatus, endoplasmic reticulum, or lysosomes. However, two ingested markers of pinocytosis, calcein and horseradish peroxidase, comigrated with the dense peak of unoxidized cholesterol. That the size of the unoxidized cholesterol pool was greater in cells deprived of serum lipoproteins than in fed cells suggested that none of the intracellular cholesterol need be ascribed to ingested sterols. The mass of unoxidizable cholesterol was not diminished when cholesterol biosynthesis was inhibited by lovastatin in lipoprotein-deprived cells. Furthermore, the newly synthesized radiolabeled cholesterol resistant to cholesterol oxidase did not migrate with intracellular cholesterol mass on sucrose density gradients. The newly synthesized cholesterol amounted to about 10% of the total unoxidized sterol. These data indicate that most of the intracellular cholesterol was not newly synthesized. We conclude that *a*) ~90% of fibroblast cholesterol is associated with the cell surface; *b*) the bulk of intracellular cholesterol, ~10% of total, is derived from internalized (endocytic) plasma membrane; and *c*) the most recently synthesized cholesterol, ~1% of the total, is in a discrete organelle. — **Lange, Y. Disposition of intracellular cholesterol in human fibroblasts.** *J. Lipid Res.* 1991. **32:** 329–339.

Supplementary key words cholesterol oxidase • organelle cholesterol • endocytosis • cholesterol biosynthesis

Cholesterol oxidase treatment of intact fibroblasts delineates two cholesterol compartments (1). Approximately 90% of cellular cholesterol is rapidly oxidized in intact cells fixed with glutaraldehyde (1). It seems reasonable to infer than at least this fraction of cellular cholesterol is in the plasma membrane. This premise has been substantiated by independent means (2). The unoxidized ~10% of the cholesterol mass has been taken to be intracellular, not only because of its failure to be oxidized but because it is rich in nascent cholesterol and free of exogenous radiocholesterol pulsed into cells (1, 3, 4).

It is generally held that cholesterol is widely distributed among the intracellular membranes (see refs. 5 and 6); however, these data have not always taken into account the contamination of subcellular fractions by plasma membrane fragments (2). If only 10% of fibroblast cholesterol is intracellular, it could be entirely accounted for by that fraction of the cell surface that is cycled through the cytoplasm by endocytosis (7). Furthermore, the contribution to the intracelluar fraction by biosynthesis on the one hand and by ingestion on the other have not been established. To address this question, we used cholesterol oxidase-treated fibroblasts to determine the disposition of intracellular cholesterol among subcellular membranes free of contamination by the substantial excess of cell surface sterol.

EXPERIMENTAL PROCEDURES

Materials

[^{3}H]Acetic acid (sodium salt, 100 mCi/mmol) and [^{14}C]acetic acid (sodium salt, 55.0 mCi/mmol) were purchased from DuPont-New England Nuclear. [1α,2α(n)-^{3}H]Cholesterol (33 Ci/mmol) and uridine diphospho-D-[6-^{3}H]galactose (ammonium salt, 17.3 Ci/mmol) were from Amersham Corp. HPLC grade solvents were obtained from Fisher. Cholesterol oxidase was obtained from Beckman Clinical Diagnostics (Carlsbad, CA).

Abbreviations: PBS, phosphate-buffered saline; HPLC, high performance liquid chromatography.

Horseradish peroxidase and 20-nm colloidal gold-labeled concanavalin A were purchased from Sigma. Lovastatin was the generous gift from Carolyn Stemmler of Merck, Sharp and Dohme Research Laboratories (West Point, PA). Lanosterol was purchased from Steraloids (Wilton, NH). The inhibitor of cholesterol biosynthesis used in Table 2 was a trace contaminant of this material, isolated by thin-layer chromatography (Y. Lange and D. G. Lynn, unpublished results). Assuming that the absorbance of the HPLC peak of the material at 214 nm was comparable to that of lanosterol itself, we estimate that <100 pg per flask inhibits the biosynthesis of fibroblast cholesterol by $\sim 80\%$ (Table 2).

Cell culture

Human foreskin fibroblasts derived from primary explants were grown in Dulbecco's modified Eagle's medium as described (3).

Labeling cell sterols

Biosynthetic labeling from radiolabeled acetate was as described (3). In order to label the cell surface with exogenous [^{3}H]cholesterol, cells in the flask were first preincubated for 5 min at 37°C with 0.05% BSA in PBS. (This treatment was found to minimize the adsorption of the radiolabel to the plastic.) [^{3}H]Cholesterol in ethanol ($<1\%$ final) was then added to the flasks and the cells were incubated for 15 min at 37°C. The buffer was removed, replaced with medium containing lipoprotein-deficient serum (8), and the flasks were incubated at 37°C for the times indicated in the figure legends.

Concanavalin A–gold density perturbation

Flasks containing confluent fibroblasts were rinsed with PBS to remove serum and the cells were incubated in a minimal volume of medium containing 0.45% bovine serum albumin and 19×10^{10} concanavalin A–gold particles/ml for 4 h at 37°C. The medium was removed and the cells were rinsed twice with PBS prior to trypsin treatment.

Treatment of cells with cholesterol oxidase and homogenization

After dissociation from the flask by trypsin treatment (3), cells were pelleted and washed sequentially in 20 volumes of 310 mM sucrose, 5 mM Na phosphate (pH 7.5) and then with 310 mM sucrose, 0.5 mM Na phosphate (pH 7.5). The cells were resuspended in approximately 8 volumes of 310 mM sucrose, 0.1 mM EDTA (pH 8.0) preequilibrated at 37°C. After a 5-min incubation at 37°C, 10 IU/ml cholesterol oxidase was added and the cells were incubated at 37°C for 10 min. (These conditions promoted maximal cholesterol oxidation.) The suspension was chilled and brought to 5 mM Na phosphate (pH 7.5), 0.3 mM $MgCl_2$ prior to homogenization on ice by 20–30 strokes in a Dounce homogenizer with a tight-fitting pestle. The homogenate was spun for 5 min at 800 g and the supernatant was retained for analysis by sucrose gradient centrifugation.

Equilibrium sucrose gradient centrifugation

Linear 11.7-ml gradients between 20% and 54% sucrose (w/v) in 5 mM Na phosphate (pH 7.5) were prepared on top of a 0.3-ml 54% sucrose cushion. The cell homogenate, typically prepared from $3–6 \times 10^6$ cells, was mixed into the gradient during its formation. The gradients were spun in a Beckman SW 41 rotor for a minimum of 10^8 g_{av}-min at 3°C. The sucrose concentration in the gradient fractions was measured by refractometry. The recovery from the gradient was $85 \pm 6\%$ and $61 \pm 18\%$ for cholestenone and cholesterol, respectively ($n = 14$).

Lipid analysis

Reverse phase HPLC of extracted lipids was carried out with a Beckman QC II system with a Model 166 programmable detector and System Gold software. An Ultrasphere ODS reversed-phase column (4.6 × 150 mm) was used with acetonitrile–isopropyl alcohol 90:10 (v/v) as the mobile phase at a flow rate of 1.5 ml/min. The effluent was monitored at 214 nm. Calibration curves for cholesterol were linear and reliable down to 0.1 μg in which range the data are given (see Fig. 1). This sensitivity is greater than in our previous studies where a different detector was used (4). A small and variable fraction of the radioactivity in the biosynthetic cholesterol peak yielded a product, after cholesterol oxidase treatment, that migrated slightly ahead of authentic cholestenone. However, the results in Fig. 5 below did not change when this contaminant was removed.

Other methods

Horseradish peroxidase was assayed by the method of Steinman and Cohn (9). Galactosyltransferase activity (10) and 5' nucleotidase activity (4) were assayed as described. Cytochrome oxidase was assayed spectrophotometrically (2).

Lysosomal hydrolase activity was measured using the fluorescent compound 4-methylumbelliferyl beta-D-galactopyranoside (Molecular Probes, Inc.) as a substrate for beta galactosidase. Aliquots from the sucrose gradients were incubated for 45 min at 37°C in a final volume of 0.25 ml containing 100 mM glycine (pH 3.0), 0.2% Triton X-100, and 0.2 mg substrate. The reaction was stopped by the addition of 7 volumes of ice-cold Na phosphate (pH 12). Fluorescence was measured at excitation and emission wavelengths of 364 nm and 450 nm, respectively.

RESULTS

Buoyant density profile of oxidized and unoxidized cholesterol

Ninety% or more of the cholesterol in cultured human fibroblasts was oxidized by treating intact cells with cholesterol oxidase (1, 3). The resulting cholestenone appeared to be associated exclusively with the plasma membrane (3, 4) and will be referred to here as such. The unoxidized fraction previously was too small to be analyzed by sucrose gradient centrifugation; however, such an analysis was performed here for the first time thanks to improvements in the sensitivity of HPLC.

Intact cells were treated with cholesterol oxidase and homogenized. Half of the homogenate was treated with digitonin to shift membranes rich in cholesterol (but not cholestenone) to a higher density (4). The two portions were spun in parallel on sucrose density gradients. The profile of cholestenone in the homogenates of cholesterol oxidase-treated cells without added digitonin had a unimodal peak at 30% sucrose, a buoyant density of 1.13 g/ml (**Fig. 1A** and ref. 4). In contrast, the unoxidized cholesterol (comprising ~5% of the total cell cholesterol in this experiment) was distributed primarily in twin peaks at 22% sucrose (d 1.09 g/ml) and 40% sucrose (d 1.18 g/ml; Fig. 1A). In numerous other experiments the denser of these two peaks was broad, and ranged between 26% and 42% sucrose (d 1.11–1.19 g/ml; e.g., Figs. 3 and 4). The relative magnitude of the two peaks varied such that the buoyant component contributed between 16–50% of the unoxidized cholesterol in 10 experiments. Fig. 1 therefore suggests that the oxidized and unoxidized pools of cholesterol reside in different membranes.

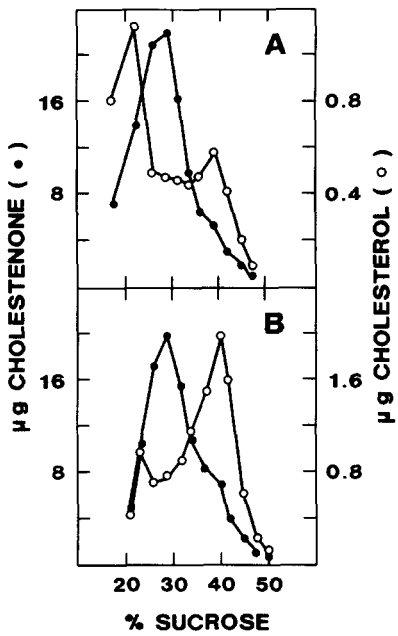

Fig. 1. The buoyant density profile of oxidized and unoxidized cell cholesterol. A suspension of fibroblasts was washed, treated with cholesterol oxidase, and homogenized as described under Experimental Procedures. The homogenate was divided into two equal aliquots, one of which was treated with digitonin as described in reference 4 while the other received ethanol alone as a solvent control. Both aliquots were spun to equilibrium on a sucrose gradient. The distribution of cholestenone (●) and cholesterol (○) was measured in the gradient fractions. Panel A, minus digitonin; panel B, plus digitonin.

Digitonin treatment had no effect on the buoyant density of the cholestenone peak (Fig. 1B; see also ref. 4). However, it caused an increase in the density of the buoyant unoxidized cholesterol peak (Fig. 1B). This suggests that those membranes are cholesterol rich (4, 11). The observation that digitonin treatment increased the density of the unoxidized cholesterol while leaving the density of cholestenone unchanged confirmed that the residual cholesterol was not associated with the plasma membrane.

The treatment of unfixed cells with cholesterol oxidase occasionally led to a small amount of cell breakdown. To determine the effect of cell breakdown on the extent of cholesterol oxidation, intact cells and homogenates were treated in parallel with cholesterol oxidase. Surprisingly, the extent of oxidation was found to be the same in both cases, even when the homogenates were exposed to glutaraldehyde, which potentiates the effect of cholesterol oxidase on plasma membranes (1). Thus, resistance to the oxidase cannot of itself be taken to signify an intracellular disposition as argued previously (1). Given that the oxidizability of membrane cholesterol has been shown to be extremely contingent on multiple factors (12, 13), the data still suggest that the membranes bearing the unoxidized sterol differ from the cell surface in some important way and are still most consistent with the intracellular disposition of the unoxidized cholesterol.

Time-dependent change in the cholesterol oxidase-susceptibility of exogenously added radiolabeled cholesterol

Plasma membranes can be labeled rapidly and selectively by a trace of radiolabeled cholesterol added to the culture medium (1). The label initially copurifies precisely with plasma membrane markers (4) and is completely oxidized by cholesterol oxidase (1); it thus is indistinguishable from the bulk of the cell surface cholesterol. We therefore used a pulse of exogenous [^{3}H]cholesterol to test whether the plasma membrane is a source of the cholesterol oxidase-resistant sterol described in Fig. 1.

Cells so labeled in culture flasks were washed, incubated at 37°C for different times, removed from the dish, fixed with glutaraldehyde, treated with cholesterol oxidase, and the specific activity of cholesterol and cholestenone was determined. The discrimination of intracellular cholesterol depended critically on minimizing residual unoxidized plasma membrane cholesterol and

correcting for this residue. When [^{3}H]cholesterol was pulsed into cells that had already been fixed, thereby blocking endocytosis and metabolically driven import, 97–99% of the total label could subsequently be oxidized by the enzyme. The observed 2% variability in oxidation was apparently not structural but due to small uncontrolled differences in experimental conditions from one day to another. Therefore, we corrected the specific activity values for each time point in all such experiments by subtracting a zero time value obtained by fixing the cells before labeling.

Fig. 2 shows the change over time of the ratio of the specific activity of unoxidized to oxidized cholesterol. The ratio increased at 37°C with a hyperbolic time course corresponding to a first order process with a half-time of ~3 h. The specific activity ratio at the plateau was 0.5. These results suggest that: *a*) the unoxidizable cholesterol pool is distinguishable from the bulk of cell cholesterol; *b*) the unoxidized pool receives cholesterol from the bulk cell surface pool; and *c*) at least half of the unoxidized cholesterol was derived from the cell surface.

When cells were incubated at 20°C, none of the exogenous radiolabeled cholesterol became resistant to cholesterol oxidase during a 3-h incubation (not shown). When such incubations were extended to 40 h at 37°C, the average ratio of specific activities rose to 0.81. The transfer of exogenous ^{3}H to a cholesterol oxidase-resistant locus thus seemed to be biphasic: approximately half proceeded with a half-time of about 3 h and the other half much more slowly. This finding also suggests that almost all of the unoxidized cholesterol mass was fed by cell surface cholesterol in a time-dependent fashion.

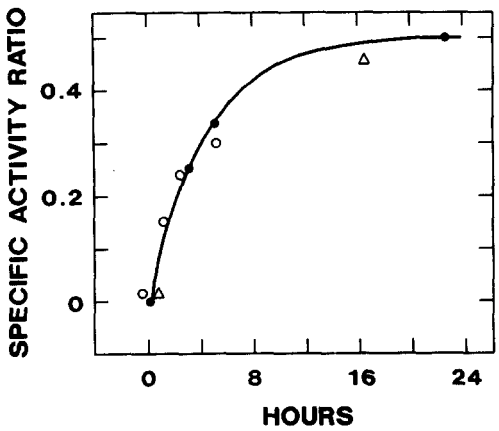

Fig. 2. Time course of transfer of exogenous radiolabeled cholesterol to a cholesterol oxidase-insensitive disposition. Confluent monolayers of fibroblasts were incubated for 48 h in medium containing 5% lipoprotein-deficient serum. The medium was replaced with unsupplemented medium containing 0.05% bovine serum albumin. After a 5-min incubation at 37°C, 5 μCi [^{3}H]cholesterol was added in ethanol to each flask. The flasks were incubated for 15 min at 37°C to label the cells. The labeled medium then was replaced with unlabeled medium supplemented with 5% lipoprotein-deficient serum and the incubation continued for the times indicated. The cells were then removed from the flask, washed, fixed with glutaraldehyde, and treated with cholesterol oxidase; the extracted lipids were analyzed by HPLC as described under Experimental Procedures. The zero time point was obtained using cells that were removed from the flask and fixed with glutaraldehyde prior to labeling with [^{3}H]cholesterol. The ordinate gives the ratio of the specific activity of the unoxidized cholesterol to that of cholestenone. Data from three experiments are plotted. Each point has been corrected for the fraction of unoxidized cholesterol at zero time. The data have been fit to the equation $y = 0.5[1 - \exp(-0.23t)]$, where 0.5 is the steady state value of y, t is the reaction time in hours, and 0.23 is the first order rate constant which corresponds to a half-time of 3 h.

A previous report suggested that exogenous radiolabeled cholesterol did not become insensitive to the oxidase with time (3). The discrepancy between that conclusion and the present findings appears to be technical in nature. Small variations in the oxidation of plasma membrane cholesterol contribute a large error to the determination of the size of the small, inherently nonoxidizable pool (5–10% of total cell cholesterol). In our earlier experiments, we added a second radioisotope of exogenous cholesterol at the end of the incubation as a reference standard to correct for variability in the oxidation of the first label, which marked plasma membrane cholesterol (3). The lack of a significant difference in the oxidation of the two labels led to the conclusion that there was no sequestration of plasma membrane cholesterol. However, we now have shown that 1–3% of the total second (reference) label became internalized during trypsin treatment at 37°C used to remove the cells from the flask. Therefore we modified the original method, adding the second isotope only after fixing the cells. This improvement allowed us to detect time- and temperature-dependent sequestration of surface label (Fig. 2).

The transfer of plasma membrane cholesterol to the intracellular cholesterol pool was previously assessed in terms of its availability for esterification; no exogenously added radiolabeled cholesterol became esterified during a 16-h incubation, during which time endogenous cholesterol was esterified (3). If the plasma membrane cholesterol that becomes oxidase-resistant is endocytic and yet not esterified, perhaps it does not reach the endoplasmic reticulum, the putative site of the acyl-CoA:cholesteryl acyltransferase (14).

Buoyant density profiles of oxidized and unoxidized exogenous radiocholesterol

The distribution of exogenous radiolabeled cholesterol in oxidizable and nonoxidizable pools was examined by isopycnic sucrose gradient centrifugation. Cells were labeled in the culture flask with a brief pulse of exogenous [^{3}H]cholesterol, washed, and incubated for 4 h at 37°C to permit internalization of the label. The cells were removed from the flask, treated with cholesterol oxidase, homogenized, and spun to equilibrium on a sucrose gradient. The distributions of the mass and radiolabel in cholestenone and cholesterol were measured throughout the gradient.

As shown in **Fig. 3A**, unoxidized [^{3}H]cholesterol co-distributed with cholesterol oxidase-resistant cholesterol mass in a bimodal profile similar to that seen in Fig. 1. However, the dense fraction of the unoxidized cholesterol invariably had a significantly higher specific activity than the buoyant fraction (Fig. 3B, open circles). The distribution of radiolabeled cholestenone ran parallel to cholestenone mass (not shown) (see ref. 4). This is indicated in Fig. 3B (closed circles) by the constancy of the specific activity of [^{3}H]cholestenone throughout the gradient. The peak specific activity of the unoxidized [^{3}H]cholesterol in this gradient ranged from 20% to 70% that of the [^{3}H]cholestenone.

The experiment shown in Fig. 3A was repeated using a 40-h incubation to allow more complete redistribution of the exogenous [^{3}H]cholesterol. In that case, the distribution of the unoxidized exogenous [^{3}H]cholesterol very closely paralleled the unoxidized cholesterol mass profile (Fig. 3C). Moreover, the specific activity of the unoxidized [^{3}H]cholesterol in both peaks was only slightly lower than the specific activity of the cholestenone (Fig. 3D). A comparison of the data obtained after 4 h (Fig. 3A) and 40 h (Fig. 3C) of incubation suggests that the surface

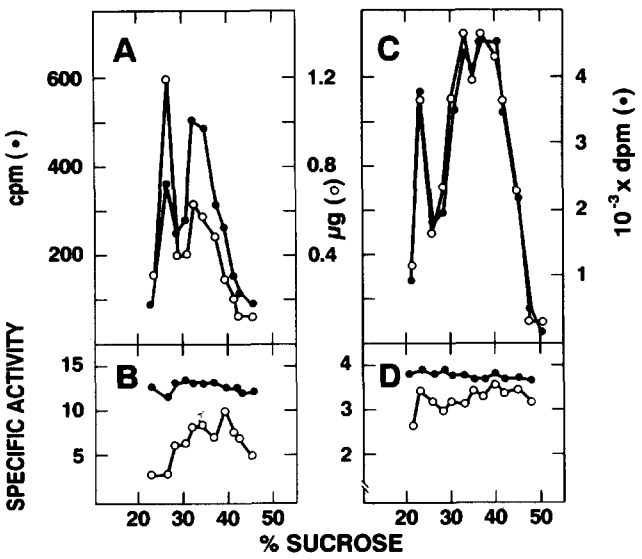

Fig. 3. The buoyant density profile of unoxidized, exogenous, radiolabeled cholesterol. Cells were labeled with exogenous [^{3}H]cholesterol in the flask as described in the legend to Fig. 2 and incubated at 37°C for 4 h (panels A and B). In a separate experiment, cells were labeled in the same way except that the 48-h preincubation in medium containing lipoprotein-deficient serum was omitted and the labeled cells were incubated for 42 h at 37°C (panels C and D). The cells were dissociated from the flasks, washed, treated with cholesterol oxidase and homogenized as described under Experimental Procedures. The homogenate was spun to equilibrium on a sucrose gradient. Panel A and C show the distribution of cholesterol mass (○) and radioactivity (●) throughout the gradient. Panels B and D show the specific activities of cholestenone (●) and cholesterol (○) expressed as 10^{-2} × cpm/μg (panel B) and 10^{-3} × dpm/μg (panel D).

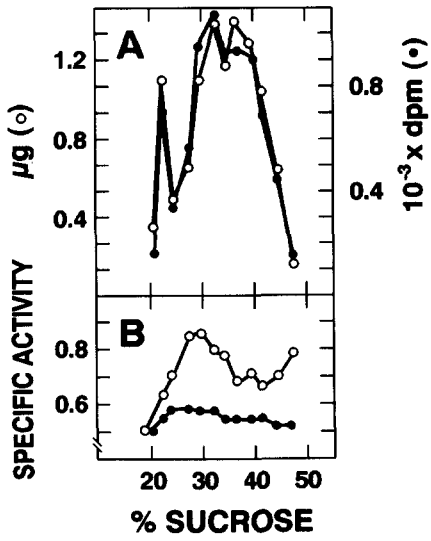

Fig. 4. The buoyant density profile of unoxidized biosynthetic cholesterol after 40 h. The experiment is the same as that shown in Fig. 3C. Two μCi/ml of [^{14}C]acetate was added to the medium immediately prior to the 42-h incubation. Panel A shows the distribution of cholesterol mass (○) and [^{14}C]radioactivity (●) throughout the gradient. Panel B shows the specific activity of [^{14}C]cholestenone (●) and [^{14}C]cholesterol (○) expressed as 10^{-3} × dpm/μg of the respective form.

cholesterol label first entered the dense membranes and only more slowly reached the buoyant membranes. These results illuminate those presented in Fig. 2 by revealing that the two peaks of unoxidizable cholesterol receive exogenous radiocholesterol with different kinetics. Furthermore, the congruence of the unoxidizable label and mass in Fig. 3C and the similarity in the specific activity of the oxidized and unoxidized pools in Fig. 3D suggest that the cell surface must be a major source of the unoxidized cholesterol.

Disposition of unoxidized endogenous cholesterol: long-term labeling

How do the pools of oxidase-resistant cholesterol relate to cholesterol synthesized by the cell? After a prolonged period of biosynthesis (42 h), endogenous [^{14}C]cholesterol (closed circles in **Fig. 4A**) closely paralleled unoxidized cholesterol mass (open circles). The specific activity of the [^{14}C]cholesterol (open circles in Fig. 4B) in this case was higher than that of the [^{14}C]cholestenone (closed circles), the converse of that observed above with labeling by exogenous [^{3}H]cholesterol (Fig. 3). The unoxidized cholesterol with the highest specific activity equilibrated at about 30% sucrose in a peak coincident with newly synthesized cholesterol (ref. 4 and Fig. 5 below). Comparing Fig. 4 with Fig. 3, we infer that endogenously synthesized cholesterol achieves a distribution among intracellular membranes that is qualitatively similar to that of exogenous cholesterol pulsed into the plasma membrane.

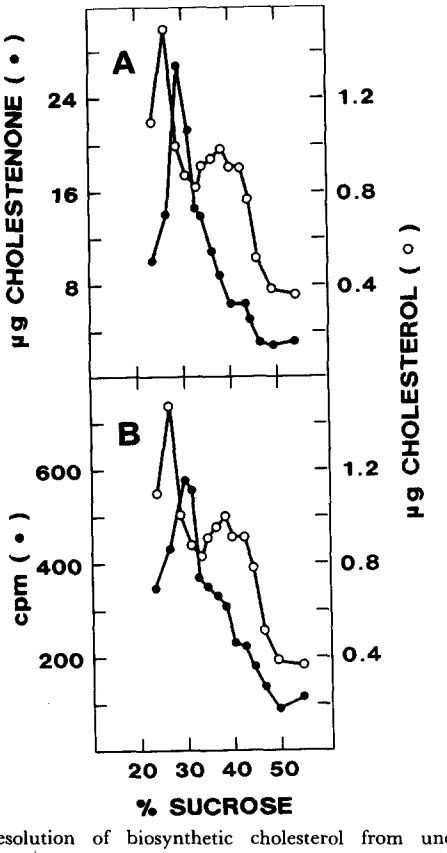

Fig. 5. Resolution of biosynthetic cholesterol from unoxidized cholesterol mass. Confluent monolayers of fibroblasts were incubated for 48 h in medium containing 5% lipoprotein-deficient serum. Bovine serum albumin was added to a concentration of 0.5% followed by concanavalin A–gold complex as described under Experimental Procedures. After a 2-h incubation at 37°C, 250 µCi[^{3}H]acetate in ethanol (<1% final concentration) was added and the cells were incubated for an additional 2 h at 37°C. The cells were dissociated from the flasks, washed, treated with cholesterol oxidase, homogenized, and spun to equilibrium on a sucrose gradient as described under Experimental Procedures. Panel A shows the cholestenone (●) and unoxidized cholesterol (○) mass profiles. Panel B shows the distribution of newly synthesized cholesterol (●) and the unoxidized cholesterol mass profile (○) replotted from panel A for comparison.

Intracellular disposition of endogenous nascent cholesterol

To examine the relationship between newly synthesized and bulk unoxidizable cholesterol, we repeated the experiment shown in Fig. 4 with a labeling period of only 2 h. The radiolabeled cholesterol now migrated as a single peak at approximately 30% sucrose (**Fig. 5B**). It appears that the intracellular pools of nascent and long-term endogenous cholesterol are not in the same membrane.

We sought additional evidence that nascent radiocholesterol and intracellular cholesterol mass were in different membranes. To better resolve the nascent cholesterol from endocytic membranes, cells were incubated for 4 h at 37°C in the presence of concanavalin A complexed with colloidal gold to selectively increase the buoyant density of endosomes (15). [^{3}H]Acetate was added to the medium for the final 2 h of this incubation to label biosynthetic cholesterol. Cell homogenates were analyzed on equilibrium sucrose density gradients. The distributions of sterol label and mass were determined throughout the gradient. Cholestenone was recovered at about 30% sucrose as before (Fig. 5, panel A). The distribution of label in cholestenone was identical to its mass (data not shown). The mass of unoxidized cholesterol was once again bimodal (Fig. 5, panels A and B). Furthermore, the dense peak of unoxidized cholesterol was shifted to a higher density than usual by the concanavalin A–gold complex. Newly synthesized cholesterol was well resolved from both peaks of unoxidized cholesterol mass (Fig. 5, panel B). These data strongly suggest that intracellular pools of nascent and chemical cholesterol are discrete and do not mix rapidly.

Quantitation of newly synthesized sterols

To estimate the size of the pool of newly synthesized intracellular cholesterol, an estimate of the specific activity of nascent sterols was first required. To obtain this value, we determined the specific activity of [^{3}H]lanosterol after 5 h of incubation with radioacetate (**Table 1**, line A). At this time, the pool of lanosterol is at the steady state (16) and its specific activity (93×10^3 cpm/µg) should be close to that of nascent cholesterol. However, given the small mass of the lanosterol pool (~0.2 µg), we were uncertain of the accuracy of such values. We therefore used an inhibitor of lanosterol demethylase isolated from a commercial preparation of lanosterol (Y. Lange and D. G. Lynn, unpublished results) to cause lanosterol to accumulate. After incubation for 5 h in medium containing lipoprotein-deficient serum plus the inhibitor, cells accumulated 1–2 µg of lanosterol mass, sufficient to be quantified accurately by HPLC (Table 1, lines B–E). The inhibitor caused the incorporation of [^{3}H]acetate into the total sterol pool to decrease slightly, while the label in lanosterol increased dramatically at the expense of that in cholesterol. The specific activity of the nascent lanosterol was (119.0 ± 7) $\times 10^3$ cpm/µg (mean of lines B–E in Table 1). The label incorporated into intracellular (unoxidized) cholesterol in a parallel control flask was 40.9×10^3 cpm (not shown). Assuming that the specific activity of nascent cholesterol is close to that of nascent lanosterol, we calculated the steady state mass of newly synthesized cholesterol in that flask to be ~0.34 µg. The nascent cholesterol therefore amounted to 0.34/44 µg or 0.8% of the total present. Note that the mass of cholesterol oxidase-resistant cholesterol is typically ten times larger than this value. The high degree of reproducibility of both cholesterol mass and lanosterol specific activity among the five flasks gives assurance of the validity of comparing flasks. Furthermore, the experiment without the inhibitor, line A, yielded a similar result. This analysis suggests that the pool of newly synthesized cholesterol is about 10% of intracellular cholesterol mass.

TABLE 1. Specific activity of newly synthesized lanosterol

Flask	Addition	Mass		^3H		Specific Activity of Lanosterol
		Cholesterol	Lanosterol	Cholesterol	Lanosterol	
		μg		$10^{-3} \times cpm$		$10^{-3} \times cpm/\mu g$
A	20 μl Ethanol	44.7	0.22[a]	268.9	20.4	93[a]
B	10 μl Inhibitor	43.8	1.08	76.0	109.9	125
C	10 μl Inhibitor	41.3	1.26	68.4	129.8	125
D	20 μl Inhibitor	44.0	1.69	50.2	168.7	114
E	20 μl Inhibitor	49.6	1.61	42.6	155.0	111

The medium of five flasks of confluent fibroblasts growing in the presence of fetal calf serum was replaced with medium supplemented with lipoprotein-deficient serum. Forty eight hours later, 0.04% bovine serum albumin and 10–20 μl ethanol containing approximately 100 pg-equivalents of the inhibitor of biosynthesis (see text) were added to four flasks. Ethanol alone was added to the fifth flask. After 10 min incubation at 37°C, 55 μCi [^{3}H]acetate was added to each flask and the cells were incubated for 5 h at 37°C. The cells were removed from the flasks, washed, fixed, treated with cholesterol oxidase, and analyzed by HPLC as described under Experimental Procedures. Values given are per flask: the mass and label in cholesterol were obtained by summing the oxidized and unoxidized ^{3}H and masses, respectively.

[a]This trace level of lanosterol mass was poorly determined; we therefore consider the specific activity of the lanosterol to be less accurate than in the presence of the inhibitor.

Organelle cholesterol

Since the data given above strongly suggest that the cell surface is not the locus of the unoxidized cholesterol, we examined the cholesterol content of major organelle fractions. Cholesterol previously has been recovered in preparations of endoplasmic reticulum, Golgi, lysosomes, and mitochondria (5).

It has been reported that the *trans* portion is richer in cholesterol than the rest of the Golgi apparatus (17) and that galactosyltransferase is a characteristic marker for this part of the Golgi stack (18). However, we found little overlap in the profiles of galactosyltransferase and the mass of unoxidized cholesterol (**Fig. 6A**). Digitonin shifted the density of the unoxidized cholesterol much more than the galactosyltransferase (Fig. 6B). These data signify that the bulk of unoxidized cholesterol is not in the same membranes as galactosyltransferase.

The equilibrium distribution of lysosomes on sucrose gradients was also examined. Sedimentable beta galactosidase with a pH optimum of 4.0 was distributed as a single peak with the buoyant density of 47% sucrose (**Fig. 7**). This is considerably more dense than unoxidizable cholesterol (Figs. 1A, 3A, and 3C). The profile of the plasma membrane marker, 5' nucleotidase, also shown in Fig. 7, was very similar to that of cholestenone mass (Figs. 1A and 5A), confirming the co-localization of these two constituents (4). Thus, although the cell surface cholesterol that becomes resistant to cholesterol oxidase appears to pass from one intracellular membrane population (30–40% sucrose) to another (25% sucrose; see Fig. 3), neither of these membranes appears to be lysosomal.

We showed previously that, under the present conditions, two putative markers for the smooth endoplasmic reticulum, cytochrome c reductase and the fraction of HMG-CoA reductase activity not associated with the nucleus, as well as ribosomal RNA, all equilibrated at greater than 40% sucrose (10), clearly denser than unoxidized cholesterol (Fig. 1). Similarly, catalase activity (a prototypic marker of the peroxisome) equilibrated in a single peak at 43% sucrose in this system (10).

We have not examined the cholesterol content of mitochondria systematically. However, we have found

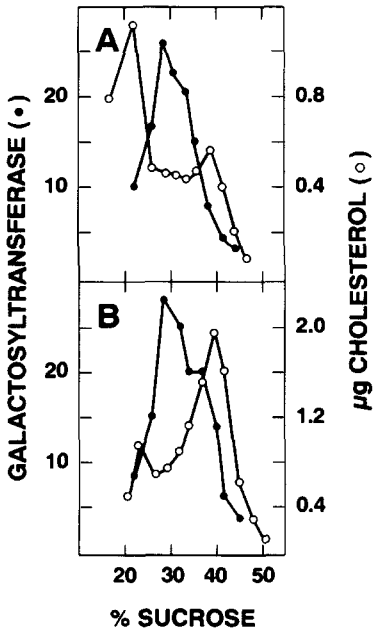

Fig. 6. Resolution of unoxidized cholesterol from galactosyltransferase activity in fibroblast homogenates. Data are from the experiment shown in Fig. 1. Galactosyltransferase activity (●) is expressed in arbitrary units in the trichloroacetic acid precipitate. Panel A, minus digitonin; panel B, plus digitonin.

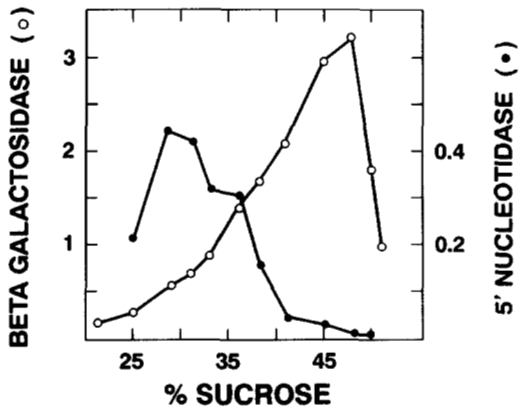

Fig. 7. The buoyant density profiles of beta galactosidase and 5' nucleotidase. Cell homogenates were spun to equilibrium on a sucrose gradient. Fractions were assayed for beta galactosidase activity (○) and 5 ' nucleotidase activity (●) as described under Experimental Procedures. Activity is expressed in relative absorbance units.

that the peak of cytochrome c oxidase activity equilibrated at 40% sucrose (not shown). Therefore, it sometimes overlapped the dense component of the biphasic cholesterol oxidase-insensitive cholesterol profile (Fig. 1). However, the mitochondrial marker sedimented far more rapidly in differential centrifugation than cholesterol oxidase-insensitive cholesterol. Furthermore, the latter (Fig. 1) but not the former was shifted in buoyant density by digitonin (see also ref. 19). Finally, mitochondria accumulated in the lower phase in two-phase aqueous partition, while the nonoxidized cholesterol favored the upper phase to about the same extent as the plasma membrane (2). Therefore, we have no evidence that any of the unoxidized cholesterol pool was borne by mitochondria in this system.

Buoyant density profile of endocytic markers

To test the hypothesis that the unoxidizable cholesterol is endocytic, we compared the isopycnic sucrose gradient distribution of this sterol with that of two water-soluble tracers of pinocytosis (reviewed in ref. 7). Cells were allowed to ingest horseradish peroxidase or calcein and then were treated with cholesterol oxidase, homogenized, and the homogenates were spun to equilibrium on sucrose gradients. As before, the major fraction of unoxidized cholesterol mass was recovered in a broad profile between 30% and 45% sucrose. The endocytic markers overlapped but did not parallel exactly the unoxidized cholesterol (**Fig. 8**).

Digitonin density shift could not be used to verify the association of the probes with the unoxidizable sterol since this agent released the sequestered markers into solution. Given that endosomes vary in time and serve to separate soluble ingested contents from plasma membrane constituents (7, 20), the lack of congruence of their profiles is not surprising. While not definitive, these data are at least consistent with the premise that most of the nonoxidizable cholesterol is endocytic.

Sources of intracellular cholesterol

The influence of serum lipoproteins on the pool of cholesterol that was unoxidizable in intact fibroblasts was analyzed. We found that cells grown in the presence and absence of lipoproteins had a similar distribution of unoxidized cholesterol on sucrose density gradients (not shown). These data indicate that lipoproteins ingested from the medium are not responsible for the profile of cholesterol oxidase-resistant cholesterol seen in Figs. 1, 4, and 8. Secondly, cells grown for 48 h in the absence of serum lipoproteins had about twice the unoxidizable cholesterol as those grown in its presence. This increase was from 5–6% to 11–12% of total cell cholesterol (**Table 2**, experiments 1 and 2). Similar observations have been made by Mazzone and Pustelniks (21). This increase in unoxidized cholesterol brought about by deprivation of lipoproteins also indicates that the contribution of ingested lipoprotein cholesterol to this pool must be small under these conditions.

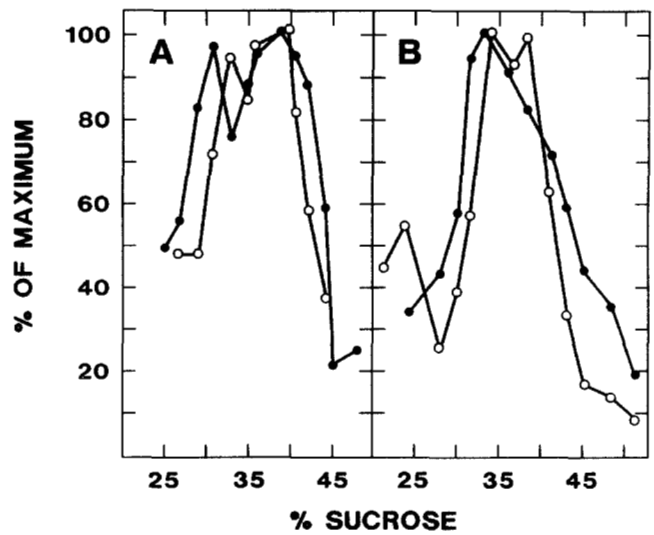

Fig. 8. Buoyant density profile of endocytic markers and unoxidized cholesterol. Panel A: Horseradish peroxidase (1 mg/ml) was added to the growth medium of confluent fibroblasts. After a 3-h incubation at 37°C, the medium was removed. The cells were covered with phosphate-buffered saline and swirled for 5 min at room temperature; this wash was repeated 5 more times. The cells then were dissociated from the flasks, washed, treated with cholesterol oxidase, and homogenized as described under Experimental Procedures. The homogenate was spun to equilibrium on a sucrose gradient. The gradient fractions were diluted with approximately nine volumes of homogenization buffer and spun for 1 h at 300,000 *g*. The pellets were resuspended in the same buffer and aliquots were taken for horseradish peroxidase assay and HPLC analysis. Horseradish peroxidase activity (●) and cholesterol mass (○) were expressed as the fraction of their maximum value. Panel B: The experiment was the same as for panel A except that the cells were incubated for 2.5 at 37°C with 1.60 mM calcein. Calcein was quantified fluorimetrically: excitation, 490 nm; emission 515 nm. Values for calcein (●) and cholesterol (○) throughout the gradient are expressed as the fraction of their maximum values.

TABLE 2. Effect of cell metabolism on intracellular cholesterol

Experiment	Medium Supplement	Addition	Oxidation	Label Incorporated
			%	*cpm*
1	Serum		95	
	LPDS		88	
2	Serum		94	
	LPDS		89	
3	LPDS	None	87	3,700
	LPDS	Lovastatin	87	0

Experiments 1 and 2: Fibroblasts in a pair of flasks were grown to confluence in the presence of fetal calf serum. The medium in one was replaced with medium supplemented with lipoprotein-deficient serum (LPDS). Forty eight hours later, the cells were removed from the flasks, washed, fixed, treated with cholesterol oxidase, and analyzed by HPLC as described under Experimental Procedures. Experiment 3: The medium in each of a pair of flasks of confluent fibroblasts grown in the presence of fetal calf serum was replaced with medium supplemented with lipoprotein-deficient serum. Five μM lovastatin was added to one flask and 2 μCi [^{3}H]acetate was added to both flasks. Forty eight hours later, the cells were treated as described above, and the incorporation of radiolabel into cholestenone and cholesterol was determined.

To examine further the contribution of newly synthesized cholesterol to the unoxidized cholesterol pool, we suppressed cholesterol biosynthesis with lovastatin, a potent inhibitor of 3-hydroxy-3-methylglutaryl-CoA reductase (22). The medium in flasks of confluent monolayers of fibroblasts was replaced with medium containing [^{3}H]acetate but lacking lipoproteins so as to stimulate cholesterol biosynthesis. Portions of the cells were incubated for 48 h in the presence and absence of 5 μM lovastatin. The incorporation of radiolabled acetate into sterols and the distribution of cholesterol between oxidizable and unoxidizable pools were then determined. The relative size of the unoxidized cholesterol fraction was found to be the same in cells incubated with and without lovastatin even though the inhibitor effectively suppressed cholesterol biosynthesis (Table 2, experiment 3). These data confirm the results shown in Fig. 5, suggesting that recently synthesized cholesterol makes a very small direct contribution to the mass of unoxidized cholesterol.

DISCUSSION

We can make the following account of the disposition of unesterified cholesterol in cultured human fibroblasts. Both by its sensitivity to cholesterol oxidase in intact cells (1) and by other analytical methods (2), ~90% of the cholesterol can be assigned to the cell surface. The residual 10% is most likely intracellular in its disposition for the following reasons. *a*) Its buoyant density profile is not that of plasma membrane markers (ref. 4 and Figs. 1 and 5). *b*) Its buoyant density profile is similar to that of endocytic markers in sucrose gradients (Fig. 8). *c*) It takes up pulses of exogenous radiolabeled cholesterol only slowly and is not in rapid exchange equilibrium with the bulk. The intracellular cholesterol compartment in this system is coincidentally resistant to cholesterol oxidase for two reasons: it is both sequestered in intact cells and unreactive in homogenates.

No one of the major organelles of fibroblasts other than the endosomes appears to contain a substantial fraction of the 10% of cell cholesterol which is cytoplasmic (2). While some studies have reported that subcellular fractions rich in endoplasmic reticulum, Golgi, lysosomes, and mitochondria typically contain demonstrable cholesterol (5), correction was not made for plasma membrane contamination in those preparations nor, in the case of lysosomes, for the ingested contents in its lumen. In the present system, most of the unoxidizable fraction of cholesterol equilibrated at a buoyant density lower than mitochondria, endoplasmic reticulum, and lysosomes. The distribution and susceptibility to digitonin of galactosyltransferase suggests that the Golgi apparatus also contains little cholesterol. By means of studies using filipin and electron microscopy (17, 23), cholesterol has been demonstrated in organelles on the endocytic pathway: coated vesicles (23), *trans* Golgi apparatus (17), lysosomes (23), and the endosomes themselves (5). However, this technique is not clearly quantitative, and is better suited to demonstrating sterol per unit area of membrane than the sterol per organelle. Nevertheless, our data are consistent with the presence of small amounts of cholesterol in these filipin-reactive membranes. Indeed, the slight increase in density (Fig. 6 and ref. 10) induced by digitonin supports this premise for the Golgi membranes.

It is conceivable that newly synthesized cholesterol passes through the Golgi apparatus on its way to the plasma membrane. However, the buoyant density profile of the bulk of the newly synthesized cholesterol differs characteristically from that of the *trans* Golgi marker, galactosyltransferase (10). Furthermore, nascent cholesterol seems to bypass the Golgi apparatus in moving to the plasma membrane (24).

Cell cholesterol ultimately derives from two sources: ingested low density lipoproteins and biosynthesis. The cholesterol of ingested lipoproteins is released to the cytoplasm by lysosomes (25); presumably, lysosomes also acquire cholesterol from internalized plasma membranes (5). However, the contribution of plasma lipoproteins to intracellular cholesterol is relatively small (Table 2), perhaps because cholesterol released from ingested lipoproteins is rapidly moved to the cell surface (26). Nascent cholesterol is observed first in intracellular membranes which are distinct from the endocytic pathway (Fig. 5). It is clear from Table 1 that this pool of nascent cholesterol contributes only a small fraction of the mass of intracellular cholesterol.

Could the major fraction of the intracellular cholesterol mass in cultured human fibroblasts derive from endocytosis of the plasma membrane? Endosomes are known to have a high cholesterol content (5). The internalization of $\geq 10\%$ of the plasma membrane by endocytosis has been suggested by earlier studies (7, 27, 28). The similarity in buoyant density between intracellular cholesterol and endocytic markers (Fig. 8) and the progressive redistribution of internalized surface [^{3}H]cholesterol (Fig. 3) suggest that the dense and buoyant peaks of unoxidizable cholesterol could correspond to early and late endosomes, respectively. The mismatch in the profiles seen in Fig. 8 might reflect the progressive sorting of the ingested soluble probes from the internal membranes (20). While endogenously synthesized sterol is found in congruence with the profile of endocytic markers after prolonged incubation (Fig. 4A), presumably it too arrived there via the plasma membrane.

Thus, the resolution of a discrete pool of endocytic cholesterol representing $\sim 10\%$ of the total is not surprising. What is notable is that endocytosed plasma membrane appears to contribute most of the mass of intracellular cholesterol. Therefore, none of the intracellular cholesterol we have analyzed appears to reside permanently within the cell; all of it is transient, coming from and going to the plasma membrane.

How is cholesterol excluded from intracellular membranes? Sterols in natural membranes may not diffuse readily through the aqueous phase (29). Instead, newly synthesized cholesterol may be moved vectorially to the cell surface through a membrane pathway (10, 24, 30). Targeted biosynthesis could explain how cholesterol avoids the endomembranes as it becomes concentrated at the cell surface (10).

Sphingomyelin is as enriched in cultured human fibroblast plasma membranes as is cholesterol; only about 10% of the sphingomyelin is intracellular (2). Since intracellular cholesterol appears to derive almost entirely from endocytic plasma membranes, it will be of interest to test to what degree the same is true of intracellular sphingomyelin.

The author would like to thank T. L. Steck for valuable discussions and critical reading of the manuscript, B. Ramos and F. Strebel for expert technical assistance, and A. Ras for typing the manuscript. This study was supported by grants HL-28448 and HL-32466 from the National Institutes of Health.

Manuscript received 5 September 1990 and in revised form 25 October 1990.

REFERENCES

1. Lange, Y., and B. V. Ramos. 1983. Analysis of the distribution of cholesterol in the intact cell. *J. Biol. Chem.* **258:** 15130–15134.
2. Lange, Y., M. H. Swaisgood, B. V. Ramos, and T. L. Steck. 1989. Plasma membranes contain half the phospholipid and 90% of the cholesterol and sphingomyelin in cultured human fibroblasts. *J. Biol. Chem.* **264:** 3786–3793.
3. Lange, Y., and H. J. G. Matthies. 1984. Transfer of cholesterol from its site of synthesis to the plasma membrane. *J. Biol. Chem.* **259:** 14624–14630.
4. Lange, Y., and T. L. Steck. 1985. Cholesterol-rich intracellular membranes: a precursor to the plasma membrane. *J. Biol. Chem.* **260:** 15592–15597.
5. Van Meer, G. 1989. Lipid traffic in animal cells. *Annu. Rev. Cell Biol.* **5:** 247–275.
6. Darnell, J., H. Lodish, and D. Baltimore. 1990. Molecular Cell Biology. 2nd Ed. Scientific American Books Inc. 493.
7. Thilo, L. 1985. Quantification of endocytosis-derived membrane traffic. *Biochim. Biophys. Acta.* **822:** 243–266.
8. Brown, M. S., and J. L. Goldstein. 1974. Suppression of 3-hydroxy-3-methylglutaryl coenzyme A reductase activity and inhibition of growth of human fibroblasts by 7-ketocholesterol. *J. Biol. Chem.* **249:** 7306–7314.
9. Steinman, R. M., and Z. A. Cohn. 1972. The interaction of soluble horseradish peroxidase with mouse peritoneal macrophages in vitro. *J. Cell Biol.* **55:** 186–204.
10. Lange, Y., and M. F. Muraski. 1988. Topographic heterogeneity in cholesterol biosynthesis. *J. Biol. Chem.* **263:** 9366–9373.
11. Boesze-Battaglia, K., T. Hennessey, and A. D. Albert. 1989. Cholesterol heterogeneity in bovine rod outer segment disk membranes. *J. Biol. Chem.* **264:** 8151–8155.
12. Pal, R., Y. Barenholz, and R. R. Wagner. 1980. Effect of cholesterol concentration on organization of viral and vesicle membranes. *J. Biol. Chem.* **255:** 5802–5806.
13. Lange, Y., H. Matthies, and T. L. Steck. 1984. Cholesterol oxidase susceptibility of the red cell membrane. *Biochim Biophys. Acta.* **769:** 551–562.
14. Hashimoto, S., and A. M. Fogelman. 1980. Smooth microsomes: a trap for cholesteryl ester in hepatic microsomes. *J. Biol. Chem.* **255:** 8678–8684.
15. Gupta, D. K., and A. M. Tartakoff. 1989. A novel lectin-gold density perturbation eliminates plasma membrane contaminants from Golgi-enriched subcellular fractions. *Eur. J. Cell Biol.* **48:** 64–70.
16. Echevarria, F., R. A. Norton, W. D. Nes, and Y. Lange. 1990. Zymosterol is located in the plasma membrane of cultured human fibroblasts. *J. Biol. Chem.* **265:** 8484–8489.
17. Orci, L., R. Montesano, P. Meda, F. Malaisse-Lagae, D. Brown, A. Perrelet, and P. Vassalli. 1981. Heterogeneous distribution of filipin-cholesterol complexes across the cisternae of the Golgi apparatus. *Proc. Natl. Acad. Sci. USA.* **78:** 293–297.
18. Dunphy, W. G., and J. E. Rothman. 1985. Compartmental organization of the Golgi stack. *Cell.* **42:** 13–21.
19. Wibo, M., D. Thines-Sempoux, A. Amar-Costesec, H. Beaufay, and D. Godelaine. 1981. Analytical study of microsomes and isolated subcellular membranes from rat liver. VIII. Subfractionation of preparations enriched with plasma membranes, outer mitochondrial membranes, or Golgi complex membranes. *J. Cell Biol.* **89:** 456–474.
20. Steinman, R. M., I. S. Melman, W. A. Muller, and Z. A. Cohn. 1983. Endocytosis and the recycling of plasma membrane. *J. Cell Biol.* **96:** 1–27.
21. Mazzone, T., and L. Pustelniks. 1990. Growth-related modulation of human skin fibroblast cholesterol distribution and metabolism. *Biochim. Biophys. Acta.* **1047:** 180–186.
22. Alberts, A. W., J. Chen, G. Kuron, V. Hunt, J. Huff, C. Hoffman, J. Rothrock, M. Lopez, M. Joshua, E. Harris, A.

Patchett, R. Monagham, S. Currie, E. Stapley, G. Albers-Schonberg, O. Hensens, J. Hirshfield, K. Hoogsteen, J. Liesch, and J. Springer. 1980. Mevinolin: a highly potent competitive inhibitor of hydroxymethylglutaryl-coenzyme A reductase and a cholesterol-lowering agent. *Proc. Natl. Acad. Sci. USA.* **77:** 3957–3961.

23. McGookey, D. J., K. Fagerberg, and R. G. W. Anderson. 1983. Filipin-cholesterol complexes form in uncoated vesicle membrane derived from coated vesicles during receptor-mediated endocytosis of low density lipoprotein. *J. Cell Biol.* **96:** 1273–1278.
24. Urbani, L., and R. D. Simoni. 1990. Cholesterol and vesicular stomatitis virus G protein take separate routes from the endoplasmic reticulum to the plasma membrane. *J. Biol. Chem.* **265:** 1919–1923.
25. Brown, M. S., and J. L. Goldstein. 1976. Receptor-mediated control of cholesterol metabolism. *Science.* **191:** 150–154.
26. Liscum, L., R. M. Ruggiero, and J. R. Faust. 1989. The intracellular transport of low density lipoprotein-derived cholesterol is defective in Niemann-Pick Type C fibroblasts. *J. Cell Biol.* **108:** 1625–1636.
27. Griffiths, G., R. Back, and M. Marsh. 1989. A quantitative analysis of the endocytic pathway in baby hamster kidney cells. *J. Cell Biol.* **109:** 2703–2720.
28. Steinman, R. M., S. E. Brodie, and Z. A. Cohn, 1976. Membrane flow during pinocytosis. *J. Cell Biol.* **68:** 665–687.
29. Steck, T. L., F. J. Kezdy, and Y. Lange. 1988. An activation-collision mechanism for cholesterol transfer between membranes. *J. Biol. Chem.* **26:** 13023–13031.
30. Kaplan, M. R., and R. D. Simoni. 1985. Transport of cholesterol from the endoplasmic reticulum to the plasma membrane. *J. Cell Biol.* **101:** 446–453.